Research Article

Synthesis, Crystal Structure, Antioxidant, Antimicrobial, and Mutagenic Activities and DNA Interaction Studies of Ni(II) Schiff Base 4-Methoxy-3-benzyloxybenzaldehyde Thiosemicarbazide Complexes

P. R. Chetana,[1] M. N. Somashekar,[1] B. S. Srinatha,[1] R. S. Policegoudra,[2] S. M. Aradhya,[3] and Ramakrishna Rao[4]

[1] Department of Chemistry, Central College Campus, Bangalore University, Bangalore 560001, India
[2] Department of Pharmaceutical Technology, Defence Research Laboratory, Tezpur 784001, India
[3] Department of Fruit and Vegetable Technology, CFTRI, Mysore 570020, India
[4] Department of Inorganic and Physical Chemistry, Indian Institute of Science, Sir CV Raman Avenue, Bangalore 560012, India

Correspondence should be addressed to P. R. Chetana; pr.chetana@gmail.com

Three new Ni(II) square planar complexes of 4-methoxy-3-benzyloxybenzaldehyde thiosemicarbazide(4m3BTSC) having polypyridyl bases of general formulation $[ML_2]$ (**1**) and [MLB] (**2**, **3**), where L = 4m3BTSC and B is N,N-donor heterocyclic bases, namely, 1,10-phenanthroline (phen, **2**), 2,2′-bipyridine (bpy, **3**), are synthesized and characterized. The free radical scavenging assay results showed that complex **1** possesses significant activity when compared to complexes **2** and **3**. The biological studies showed that the ligand and its complexes exhibited significant and different biological activities and also the prepared compounds are nonmutagenic. They may be potential commercial antioxidants because of their nonmutagenic and nontoxic nature. The DNA interaction of the new complexes is evaluated by absorption, emission, and melting temperature methods, and the results suggested that the binding affinity of the complexes increases with the presence of planar ligand in the molecule. The nickel (II) complexes with planar phenanthroline bases show moderate DNA binding and cleavage ability.

1. Introduction

Schiff bases have great importance in coordination chemistry due to their ability to form a range of complexes with applications in different fields [1]. Thiosemicarbazones have variable bonding modes, ability to form stable chelates with metal ions, and structural diversity [2]. The sulfur, oxygen, and nitrogen may be involved in coordination providing a useful model for bioinorganic processes [3]. These thiosemicarbazide ligands have good complexing ability, and their activity increases on complexation with transition metal ions [4]. These compounds are also of interest due to their biological activities including enzyme inhibition [5] and antifungal and pharmacological applications [6, 7]. The toxicological importance of the –N–C=S moiety has been well established

in antifungal, antibacterial agents and pesticidal activities [8, 9]. It has been suggested that the azomethine linkage in Schiff bases is responsible for the biological activities such as antitumor, antibacterial, antifungal, and herbicidal activities [10].

The biological activities of thiosemicarbazones often showed a high dependence on their substituents. Minor modifications in the structure of thiosemicarbazones can lead to widely different biological activities. The biological properties of thiosemicarbazones are often modulated by metal coordination. In some cases, the highest biological activity is associated with a metal, and some side effects may decrease upon complexation [11].

Nickel(II) complexes have found several potential applications in medicine, and very recently they have been

screened for inhibition of cancer cell proliferation [12, 13]. In the last 20 years transition metal complexes have become increasingly important as drugs and artificial nucleases. One goal of designing Ni(II) complexes is developing more reactive chemical systems that can efficiently cleave DNA under physiological conditions [14–16].

Substantial progress has been made during the past few decades to develop metal-based small molecules as DNA foot-printing as well as the therapeutic agents that are capable of binding and cleaving DNA under physiological condition [17, 18]. Among the metal complexes so far investigated, those of polypyridyl phenanthroline bases have attracted great attention by virtue of its binding propensity to nucleic acid under the physiological condition [19, 20].

In view of the varying ligation behavior and interesting biological activity shown by these nitrogen-sulfur ligands and their complexes, we are also interested to prepare the thiosemicarbazide Schiff base and its metal complexes. Designing of these metal complexes has been undertaken, and their biological activities have been studied. The study of biological activities of benzyloxy benzaldehyde-Schiff bases is less explored. Herein, we present the syntheses, structure, antioxidant, antimicrobial, and mutagenic activities and DNA interactions of nickel(II) complexes of general formulae $[Ni(L)_2]$ (**1**), $[Ni(L)(B)]$ (**2**, **3**) where L is ligand 4m3BTSC (4-methoxy-3-benzyloxybenzaldehyde thiosemicarbazide) and B is N,N-donor heterocyclic base, namely, 1,10-phenanthroline (phen), 2,2′-bipyridine (bpy).

2. Experimental

2.1. Materials and Instrumentation. All reagents and chemicals were of AR grade and used as purchased. The 4-methoxy-3-benzyloxy benzaldehyde, thiosemicarbazide, and various metal salts were Merck products and used as supplied. The agarose (molecular biology grade) and ethidium bromide (EB) were obtained from Sigma. Calf thymus (CT) DNA and Supercoiled (SC) pUC19 DNA (cesium chloride purified) were purchased from Bangalore Genie (India). The tris(hydroxymethyl)-aminomethane-HCl (tris-HCl) buffer was prepared by doubly distilled H_2O.

Bacterial Strains. The four *Salmonella typhimurium* mutant strains (histidine-dependant) TA98, TA100, TA1535, and TA1538 were procured from IMTECH, Chandigarh, India. For mutagenicity assay, each bacterial culture was inoculated in 10 mL of fresh nutrient broth and incubated at 37°C for 14 h. All chemicals and bacterial media were purchased from Himedia.

The elemental analyses were carried out by using vario-micro CHNS15106062 analyzer. ^{1}H NMR and ESI-MS data of the compounds were recorded at the Sophisticated Analytical and Instrument Facility, IISc, Bangalore. The IR spectra of the samples were recorded on a Shimadzu spectrophotometer from 4000 to 400 cm^{-1} using KBr pellets. The UV-Vis spectra were recorded on a Shimadzu UV-3101PC spectrophotometer using DMF as solvent. The molar conductances of

the complexes were measured using Equiptronics digital conductivity meter number EQ-660A, and the melting points were checked by melting point apparatus used in laboratories. Magnetic susceptibility data at 300 K for the polycrystalline samples of the complexes were obtained by VSM, IIT Madras.

2.2. Synthesis. The Schiff base ligand 4m3BTSC was synthesized by reported procedure [21].

*2.2.1. Preparation of $[Ni(L)_2](X)$ (**1**) (L = 4m3BTSC, X = DMF) and $[Ni(L)(B)]$ (**2**, **3**) (B = phen, bpy) Complexes.* The complexes were prepared by following a modified reported [22] synthetic procedure in which a 10 mL methanolic solution of $Ni(CH_3COO)_2 \cdot 4H_2O$ (0.24 g, 1 mmol) was reacted with 4m3BTSC (0.315 g, 1 mmol) in acetonitrile (10 mL) under magnetic stirring at room temperature. The resulting precipitate was filtered off, washed with methanol, and air-dried. The obtained precipitate was dissolved in dimethyl formamide and leaving it to stand for a week on slow evaporation of the solution at room temperature yielded a crystalline material (**1**). Crystals of complexes were suitable for X-ray diffraction studies. After 30 min, a 20 mL methanolic solution of the heterocyclic base [phen (0.198 g, 1 mmol) bpy (0.156 g, 1 mmol)] was added to the solution, and the resulting mixture was stirred for 2 h at room temperature. On cooling the solution to an ambient temperature, it was filtered and the filtrate on slow concentration yielded a crystalline solid of the product (**2**, **3**). The solid was isolated and washed with cold methanol and finally dried over P_4O_{10}. The FT-IR, 1H NMR and ESI-MS spectras for all the complexes are given in supplementary material (Figures S1–S9).

Analyses Calculaed for Complex 1 ($C_{32}H_{34}N_6NiO_4S_2$). CHNS Analyses Calc: C, 55.74; H, 4.99; N, 12.19; S, 9.60; found: C, 53.13; H, 5.05; N, 13.03; S, 9.43%. FT-IR; cm^{-1}, (KBr disc): 3420 m (NH_2), 3180 m (N–H), 1596 s (C=N), 1522 m (C=C), 1020 m (–N–N), 800 m (C=S), 466 m (Ni–N), cm^{-1}, for complex **1**: λ_{max} /nm (ε/dm^3 M^{-1} cm^{-1}) in DMF: 532(490), 438(580), 370(1600), 340(2220), 285(1230), 268(23833), μ_{eff} (solid, 300 K): 0.41 μB, Λ_M (Ω^{-1} cm^2 M^{-1}) in DMF at 25°C: 11.7, ESI-MS; 688.01.

Analyses Calculaed for Complex 2 ($C_{28}H_{25}N_5NiO_2S$). CHNS Analyses, Calc: C, 60.67; H, 4.55; N, 12.63; S, 5.79; found: C, 61.32; H, 4.88; N, 12.82; S, 5.81%. FT-IR; cm^{-1}, (KBr disc): 3420 m (NH_2), 3180 m (N–H), 1600 s (C=N), 1522 m (C=C), 1020 m (–N–N), 817 m (C=S), 455 m (Ni–N), cm^{-1}, λ_{max}/nm (ε/dm^3 M^{-1} cm^{-1}) in DMF: 530(470), 434(700), 370(1550), 338(2520), 272(2530). (solid, 300 K): 0.30 μB, Λ_M (Ω^{-1} cm^2 M^{-1}) in DMF at 25°C: 9.2, ESI-MS; 553.7.

Analyses Calculaed for Complex 3 ($C_{26}H_{25}N_5NiO_2S$). CHNS Analyses, Calc: C, 58.89; H, 4.75; N, 13.21; S, 6.05; found: C, 59.01; H, 4.96; N, 13.22, S, 6.31%. FT-IR; cm^{-1}, (KBr disc): 3420 m (NH_2), 3180 m (N–H), 1600 s (C=N), 1522 m (C=C), 1020 m (–N–N), 810 m (C=S), 455 m (Ni–N), cm^{-1}, λ_{max}/nm (ε/dm^3 M^{-1} cm^{-1}) in DMF: 528(530), 435(860),

375(2260), 338(2870), 268(2450), μ_{eff} (solid, 300 K): 0.40 μB, Λ_M (Ω^{-1} cm^2 M^{-1}) in DMF at 25°C: 8.4, ESI-MS; 529.6.

2.3. X-Ray Crystallographic Procedures.
Single crystal of the complex **1** was grown by slow evaporation of DMF solution. Darkgrey single crystal was mounted on a glass fiber with epoxy cement. The X-ray diffraction data were measured in frames with increasing ω (width of 0.3° per frame) and with a scan speed at 15 s/frame on a Bruker SMART APEX CCD diffractometer, equipped with a fine focus 1.75 kW sealed tube X-ray source. Empirical absorption corrections were carried out using multiscan program [23]. The structure was solved by the heavy atom method and refined by full matrix least-squares using SHELX system of programs [24].

2.4. Antioxidant Activity

2.4.1. 2,2-Diphenyl-1-picryl-hydrazyl (DPPH•) Radical Scavenging Method.
The reduction capability of DPPH radicals was determined by the decrease in its absorbance at 517 nm which can be induced by antioxidants [25]. Antioxidant activity of ligand and metal complexes was determined by the method described by Brand-Williams et al. [26]. The complex solutions (100 μL, 1 mmol) were mixed with 0.8 mL of tris-HCl buffer (pH 7.4) to which 1 mL of DPPH• (500 μM in ethanol) was added. The mixture was shaken vigorously and left to stand for 30 min. Absorbance of the resulting solution was measured at 517 nm in a Uv-Vis Spectrophotometer. The radical scavenging activity was measured by decrease in the absorbance of DPPH. Lower absorbance of the reaction mixture indicated higher free radical scavenging activity.

2.5. Antimicrobial Activity.
The antibacterial activity was tested against clinical isolates like *Bacillus subtilis*, *Micrococcus luteus, Staphylococcus aureus, Klebsiella pneumoniae, Escherichia coli,* and *Pseudomonas aeruginosa.* The test organisms were maintained on nutrient agar slants. *In vitro* antibacterial activity was determined by the agar well-diffusion method as described by Mukherjee et al. [27]. The overnight bacterial culture was centrifuged at 8000 rpm for 10 min. The bacterial cells were suspended in saline to make a suspension of 10^5 CFU/mL and used for the assay. Plating was carried out by transferring the bacterial suspension to a sterile Petri plate and mixed with molten nutrient agar medium, allowing the mixture to solidify. About 75 μL of the sample (2 mg/mL) was placed in the wells. Plates were incubated at 37°C, and activity was determined by measuring the diameter of the inhibition zones. The assay was carried out in triplicate.

2.6. Mutagenicity Assay.
Mutagenicity of compounds was studied by the preincubation assay as described by Maron and Ames [28]. 100 μL of fresh culture of *Salmonella* strains was treated with test compounds dissolved in DMSO with concentrations of 2, 5, and 10 mg/plate at 37°C. For the mutagenicity assay, the controls and compound-treated cells were mixed with 2 mL of sterile top agar and poured onto minimal glucose agar plate. The plates were then inverted and incubated at 37°C for 48 hrs. Revertant colonies of bacteria

were counted manually after 48 h. Each experiment consisted of three replicates for each concentration.

2.7. DNA Binding Experiments.
The UV absorbance at 260 and 280 nm of the CT-DNA solution in 5 mM tris-HCl buffer (pH 7.2) gave a ratio of 1.9, indicating that the DNA was free of protein [29]. The concentration of CT DNA was measured from the band intensity at 260 nm with a known ε value (6600 M^{-1} cm^{-1}) [30]. Absorption titration measurements were done by varying the concentration of CT DNA, keeping the metal complex concentration constant in 5 mM tris-HCl/5 mM NaCl buffer (pH 7.2). Samples were kept for equilibrium before recording each spectrum. The intrinsic binding constant (K_b) for the interaction of the complexes with CT-DNA was determined from a plot of $[\text{DNA}]/(\varepsilon_a - \varepsilon_f)$ versus [DNA] using absorption spectral titration data and the following equation:

$$\frac{[\text{DNA}]}{\left(\varepsilon_a - \varepsilon_f\right)} = \frac{[\text{DNA}]}{\left(\varepsilon_b - \varepsilon_f\right)} + \left[K_b\left(\varepsilon_b - \varepsilon_f\right)\right]^{-1}, \qquad (1)$$

where [DNA] is the concentration of DNA in base pairs. The apparent absorption coefficients ε_a, ε_f, and ε_b correspond to $A_{\text{obsd.}}/[\text{Ni}]$, the extinction coefficient for the free nickel(II) complex, and extinction coefficient for the nickel(II) complex in the fully bound form, respectively [31]. K_b is given by the ratio of the slope to the intercept.

The apparent binding constant (K_{app}) of the complexes was determined by fluorescence spectral technique using ethidium bromide (EB) bound CT DNA solution in tris-HCl/NaCl buffer (pH 7.2). The fluorescence intensities of EB at 600 nm (546 nm excitation) with an increasing amount of the ternary complex concentration were recorded. Ethidium bromide was nonemissive in tris-buffer medium due to fluorescence quenching of the free EB by the solvent molecules [32, 33]. In the presence of DNA, EB showed enhanced emission intensity due to its intercalative binding to DNA. A competitive binding of the copper complexes to CT DNA could result in the displacement of EB or quenching of the bound EB by the paramagnetic nickel(II) species decreasing its emission intensity.

DNA-melting experiments were carried out by monitoring the absorbance of CT-DNA (200 μM NP) at 260 nm with varying temperature in the absence and presence of the complexes in 2 : 1 ratio of DNA to complex with a ramp rate of 0.5°C min^{-1} in phosphate buffer (pH 6.85) using a Peltier system attached to the UV-Vis spectrophotometer.

2.8. DNA Cleavage.
The extent of cleavage of supercoiled (SC) DNA in the presence of the complex and oxidizing agent H$_2$O$_2$ was determined by agarose gel electrophoresis. In a typical reaction, supercoiled pUC19 DNA (0.2 μg), taken in 50 mM tris-HCl buffer (pH 7.2) containing 50 mM NaCl, was treated with the complex. The extent of cleavage was measured from the intensities of the bands using UVITEC Gel Documentation System. For mechanistic investigations, inhibition reactions were done on adding the reagents prior to the addition of the complex. The solutions were incubated

TABLE 1: Analytical and physical data of the ligand and its complexes.

Complex	1	2	3
Colour, [a]MP/°C	Dark brown, 190	Cream, 195	Cream, 195
[b]IR $(cm^{-1})/\nu(C=N) + \nu(C=S)$	1596, 800	1600, 817	1600, 810
[c]d-d band (nm)	532	530	530
[d]$\Lambda_M/\Omega^{-1}cm^2mol^{-1}$	11.7	9.2	8.4
[e]μ_{eff}	0.3	0.4	0.4

[a]Melting point, [b]KBr Phase, [c]in DMF medium, [d]in DMF medium at 25°C, and [e]μ_{eff} for solid at 300 K.

for 1 h in a dark chamber at 37°C followed by addition to the loading buffer containing 25% bromophenol blue, 0.25% xylene cyanol, and 30% glycerol ($2\,\mu L$), and the solution was finally loaded on 0.8% agarose gel containing $1.0\,\mu g/mL$ ethidium bromide (EB). Electrophoresis was carried out for 2 h at 60 V in tris-acetate-EDTA (TAE) buffer. Bands were visualized by UV light and photographed for analysis. Due corrections were made to the observed intensities for the low level of NC form present in the original sample of SC DNA and for the low affinity of EB binding to SC in comparison to nicked-circular (NC) and linear forms of DNA [34].

3. Results and Discussion

3.1. Synthesis and General Aspects.

The new nickel(II) complexes are prepared in high yield from the reaction of $Ni(CH_3COO)_2\cdot 4H_2O$ with ligand 4m3BTSC and heterocyclic bases. The complexes were soluble in DMF, DMSO and sparingly soluble in acetonitrile, chloroform, and dichloromethane. The analytical data correspond well with the general formula $[ML_2]$ (DMF) (**1**) or [MLB], where M is nickel, L = 4m3BTSC, and B is 1,10-phen, 2,2-bpy (**2**, **3**). The proposed structures of complexes **2** and **3** are given in Figure 1. The molar conductance values of 1 mM solutions of the metal complexes in DMF at room temperature are in the range of $8-12\,\Omega^{-1}cm^2\,mol^{-1}$, indicating their nonelectrolytic nature [35]. They are characterized from the analytical and physicochemical data (Table 1). The complexes **2** and **3** display an intense charge transfer (CT) band in the range 200–310 nm, which can be attributed to the $\pi \rightarrow \pi^*$ transition of the coordinated N,N-donor heterocyclic base. The band around 330 and 340 nm in all the complexes is due to the imine (–HC=N–) and C=S groups, and the occurrence of two d-d bands in the regions 527–538 and 430–438 nm ($^1A_1g\rightarrow{}^1B_2g$ and $^1A_1g\rightarrow{}^1B_1g$ transitions) is consistent with a square planar structure for all the all complexes.

3.2. Crystal Structure of 1.

The $Ni(L)_2$ (DMF) complex is structurally characterized using single-crystal X-ray diffraction technique. The ORTEP diagram and numbering scheme for $Ni(L)_2$ are shown in Figure 2. Crystallographic data for complex **1** is presented in Table 2. X-ray studies reveal that the complex has square planar geometry as is evident from their bond parameters and bond angles (Table 3). Complex **1** crystallizes in the centrosymmetric P2$_1$/n space group of the monoclinic crystal system with cell parameters, $a = 15.669(5)$ Å, $b = 9.127(5)$ Å, $c = 16.227(5)$ Å, and

TABLE 2: Crystallographic data for NiL_2(**1**) complex.

Formula	$C_{32}H_{24}N_6NiO_4S_2$
Formula weight	688.40
Crystal system, space group	Monoclinic, P2$_1$/n
a, b, c(Å)	15.669(5), 9.127(5), 16.227(5)
$\alpha°, \beta°, \gamma°$	90, 116.2(5), 90
V (Å^3), Z	2081.4(15), 4
T (K)	293
θ	23.8°
μ	1.20 mm^{-1}
λ (Å) (Mo Kα)	0.71073
D_x	2.168 Mg m^{-3}
Refinement method	Full-matrix least-squares on F^2
Goodness of fit on F^2	1.07
R_{int}	0.027
Final R indices	$wR(F^2) = 0.134$

TABLE 3: Selected bond lengths (Å) and bond angles (°) for NiL_2(**1**) complex.

Ni1–N1^i	1.937(2)	N1–N2	1.386(3)
Ni1–N1	1.937(2)	N2–C16	1.295(4)
Ni1–S1	2.1614(11)	N3–C16	1.335(4)
Ni1–S1^i	2.1614(11)	N4–C19	1.323(7)
S1–C16	1.716(3)	N4–C18	1.384(7)
N1^i–Ni1–N1	180.00(9)	C18–N4–C17	122.0(7)
N1^i–Ni1–S1	94.26(8)	O1–C6–C7	108.3(3)
N1–Ni1–S1	85.74(8)	O1–C8–C9	124.7(3)
N1^i–Ni1–S1^i	85.74(8)	O1–C8–C13	114.6(3)
N1–Ni1–S1^i	94.26(8)	C9–C8–C13	120.7(3)
S1–Ni1–S1^i	180.00(4)	C8–C9–C10	120.3(3)
C16–S1–Ni1	97.15(11)	O2–C13–C12	125.4(3)
C8–O1–C6	117.2(2)	O2–C13–C8	115.0(3)
C13–O2–C14	118.0(2)	C12–C13–C8	119.5(3)
C15–N1–N2	114.2(2)	N1–C15–C10	133.4(3)
C15–N1–Ni1	125.8(2)	N2–C16–N3	119.6(3)
N2–N1–Ni1	119.96(19)	N2–C16–S1	122.8(2)
C16–N2–N1	113.9(2)	N3–C16–S1	117.6(2)
C19–N4–C18	119.3(7)	O2–C13–C12	125.4(3)
C19–N4–C17	118.7(5)	O2–C13–C8	115.0(3)

$V = 2081.4(15)$ Å^3. All nonhydrogen atoms were refined anisotropically, and the hydrogen was refined isotropically.
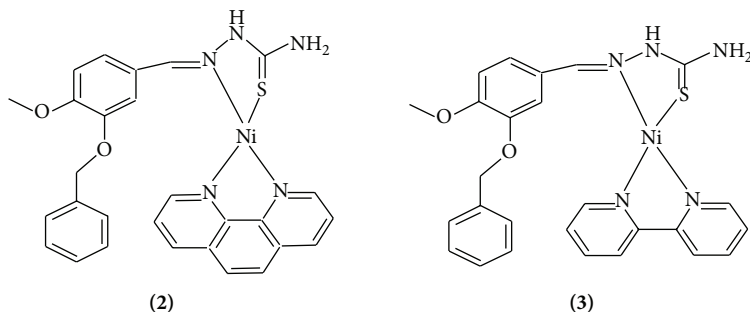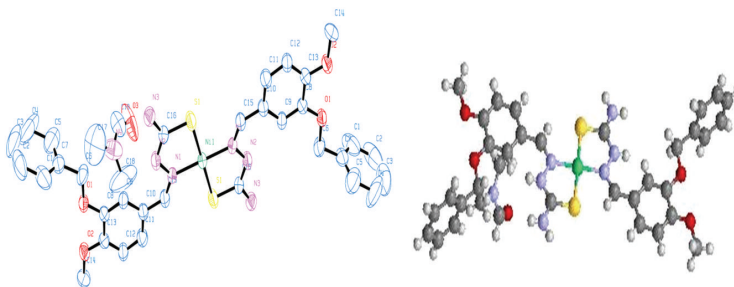
FIGURE 1: Proposed structures of Ni(II) complexes **2** and **3**.

FIGURE 2: The ORTEP and ball and stick view of the complex $Ni(L)_2$ (DMF) (**1**).

The hydrogen atoms attached to the heteroatoms were in their calculated positions and refined according to the riding model. The coordination polyhedron around the nickel atom is best described as square planar with an N_2S_2 donor set. The nickel atom is located at the centre of symmetry and is coordinated by two sulphur atoms and two azomethine nitrogen atoms from two Schiff base ligands in usual trans arrangement. The trans bond angle of N(1)–Ni–N(1) is exactly 180°, and the bond angle between S(1)–Ni–S(1) is also 180°, this confirms that structure is square planar. The crystal packing viewed along the cell axis displays nine independent molecules accommodated in the crystallographic asymmetric unit in which eight molecules occupy eight corners of the unit cell and one more molecule is occupied in the centre of the unit cell. The structure shows extensive intermolecular noncovalent interactions, and it is also stabilized by N–H···O intermolecular hydrogen bonding. Here the atom N3 acts as a donor to O atom of the lattice DMF molecule (distance: 2.678 Å). The unit cell packing diagram present in complex **1** is shown in Figure 3(a), and the intermolecular hydrogen bonding is shown in Figure 3(b).

3.3. IR Spectra. In principle, the ligand can exhibit thione-thiol tautomerism since it contains a thioamide –NH–C=S functional group. The ν(S–H) band at 2565 cm^{-1} is absent in the IR spectrum of ligand, but ν(N–H) band at ~3265 cm^{-1} is present, indicating that in the solid state the ligand remains as the thione tautomer. The position of ν(C=N) band of the thiosemicarbazone appeared at 1616 cm^{-1} is shifted towards lower wave number in the complexes indicating coordination via the azomethine nitrogen. This is also confirmed by

the appearance of band in complexes in the range of 450–455 cm^{-1}, which has been assigned to the ν(M–N) [36]. A medium band found at 1014 cm^{-1} is due to the ν(N–N) group of the thiosemicarbazone. The position of this band is shifted towards higher wave number in the spectra of complexes. It is due to the increase in the bond strength, which again confirms the coordination via the azomethine nitrogen. The band appearing at ~830 cm^{-1} corresponding to ν(C=S) in the IR spectrum of ligand is shifted towards lower wave number. It indicates that thione sulfur coordinates to the metal ion [37]. Thus, it may be concluded that the ligand behaves as bidentate chelating agent coordinating through azomethine nitrogen and thiolate sulfur. The C–H stretching and bending vibrations appear at 2780–2890 cm^{-1} and 1460–1420 cm^{-1}, respectively.

3.4. ^1H NMR Spectra. The ^{1}H NMR spectra of ligand and its nickel complexes were recorded in CDCl$_3$. The ^{1}H NMR spectrum of 4m3BTSC shows signal at 8.30 δ indicating the presence of azomethine (HC=N) proton. The singlet peaks between 9.3–10.1 δ and ~6.8 δ are assigned for the presence of NH and NH$_2$ protons; however the multiplet in the region 7.10–7.6 δ indicates the presence of the phenolic protons. No signals are observed in the range 11.3-11.4 δ which indicates the absence of thiol (–SH) group. The other important bands were observed at ~3.9 δ assigned for methyl (O–CH$_3$) protons and 5.16 δ assigned for methylene (O–CH$_2$) protons. The azomethine proton in the Ni(II) complexes is shifted downfield compared to free ligand, suggesting deshielding of the azomethine group due to coordination with nickel.
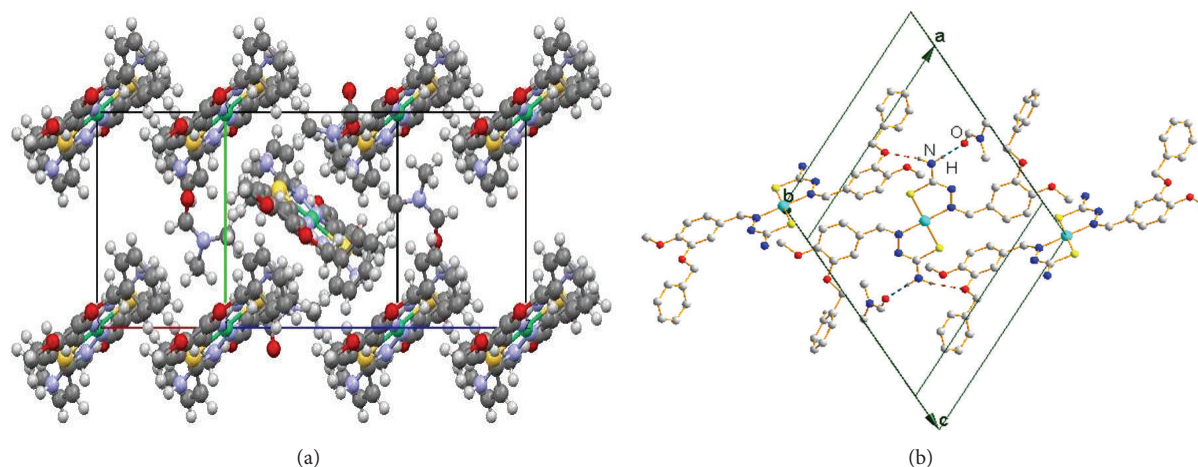
(a)

(b)

FIGURE 3: (a) Molecular packing for the complex NiL$_2$, viewed down the c-axis; (b) dashed lines indicate hydrogen bonds.

TABLE 4: ^{1}H NMR spectra of ligand and its complexes.

Compounds	−NH (δ)	−CH=N− (δ)	−Ph− (δ)	−NH$_2$ (δ)	−CH$_2$, −OCH$_3$ (δ)
4m3BTSC	10.07 (s, 1H, NH)	8.30 (s, 1H)	7.1–7.4 (m)	8.02 (s, 2H, NH$_2$)	5.16 (s, 2H, CH$_2$) 3.90 (s, 3H, CH$_3$)
1	10.1 (s, 1H, NH)	7.81 (s, 1H)	7.2–7.4 (m)	6.88 (s, 2H, NH$_2$)	5.16 (s, 2H, CH$_2$) 3.90 (s, 3H, CH$_3$)
2	8.9 (s, 1H, NH)	7.97 (s, 1H)	7.2–7.4 (m)	6.82 (s, 2H, NH$_2$)	5.16 (s, 2H, CH$_2$) 3.90 (s, 3H, CH$_3$)
3	8.9 (s, 1H, NH)	7.64 (s, 1H)	7.2–7.4 (m)	6.88 (s, 2H, NH$_2$)	5.16 (s, 2H, CH$_2$) 3.90 (s, 3H, CH$_3$)

s: singlet and m: multiplet.

TABLE 5: DPPH radical scavenging activity of complexes **1**, **2**, and **3** and standards.

Compounds	Conc. (μM)	^{a}EC$_{50}$	^{b}ARP	^{c}AE
4m3BTSC	—	NI	NI	NI
1	40	0.110	6.2	3.47×10^{-3}
2	50	0.110	5.0	2.7×10^{-3}
3	50	0.105	5.2	2.9×10^{-3}
Vit-C	42	0.168	8.3	4.6×10^{-3}
BHT	20	0.08	12.5	6.9×10^{-3}

NI: no inhibition, ^{a}EC$_{50}$: effective concentration = μM conc. of antioxidant/μM conc. of DPPH.
^{b}ARP: antioxidant radical power = 1/EC$_{50}$.
^{c}AE: antioxidant efficiency = 1/EC$_{50}$ $T_{EC_{50}}$.
Vit-C: vitamin C.
BHT: butylated hydroxy anisole.

There is no appreciable change in the other signals of the complexes (Table 4).

3.5. Antioxidant Activity

3.5.1. DPPH Radical Scavenging Activity. Various researchers have used scavenging effect of a chemical on DPPH radical as a quick and reliable parameter to assess the *in vitro* antioxidant activity. The efficient concentration of complex required to scavenge 50% of DPPH, EC$_{50}$, is shown in Table 5. The lower the EC$_{50}$ is, the better its radical scavenging activity is. It is evident from results that free radical scavenging activities of these compounds were concentration dependent. Among the examined compounds, the complex **1** showed a strong interactive ability with DPPH, expressed as EC$_{50}$ value of 40 μM concentration, which was close to that of ascorbic acid (30 μM). Maximum free radical scavenging activity (56.9%) was found in complex **1** followed by complex **3** (52.41%) and complex **2** (51.8%), while least activity (32.88%) was observed for free ligand 4m3BTSC. The comparative time-dependent antioxidant activity of compounds and standards were shown by graph in Figure 4. Antiradical efficiency (AE) involves the potency (1/EC$_{50}$) and the reaction time ($T_{EC_{50}}$). The AE of all the complexes are in the range of 2.5–3.5 $\times 10^{-3}$, the value near to standards and the complexes are good antioxidants [38].

3.6. Antibacterial Activity. The *in vitro* antibacterial activity of the Schiff bases and their Ni(II) complexes were evaluated against three Gram positive, *S. aureus, B. subtilis*, and *M. luteus,* and three Gram negative bacteria, *P. aeruginosa, K. pneumoniae,* and *E. coli*. Table 6 illustrates the antimicrobial activity of the synthesized compounds. In general, the synthesized Schiff bases have more antibacterial activity compared to their metal complexes; this may be due to

TABLE 6: The values of zone inhibition (mm) of microorganisms for the 4m3BTSC and its complexes **1**, **2**, and **3**.

Bacteria	4m3BTSC	**1**	**2**	**3**
E. coli (MTCC 443)	10	10	12	—
P. aeruginosa (MTCC 741)	—	—	11	—
K. pneumonia (MTCC 109)	12	—	14	10
B. subtilis (MTCC 441)	12	10	15	9
M. luteus (MTCC 106)	11	—	12	—
S. aureus (MTCC 3160)	—	—	12	—

the greater liphophilic nature of the Schiff bases than their metal complexes. The results showed that the complex **2** exhibited antibacterial activity against all the tested organisms, namely, *E. coli*, *P. aeruginosa, K. pneumoniae, B. subtilis, M. luteus,* and *S. aureus*. The result also indicated that the complex **1** exhibited antibacterial activity against *E. coli* and *B. subtilis* and that complex **3** exhibited antibacterial activities against *K. pneumonia* and *B. subtilis,* respectively. The factors that govern antimicrobial activities are strongly dependent on the central metal ion and coordination numbers and are also due to the presence of nitrogen and sulfur donor groups [39, 40].

3.7. Mutagenic Assay. The mutagenic activity was carried out by Ames test. The results indicate that all the complexes are nonmutagenic in nature under assay condition. According to the Ames test, the tested ligand and its complexes did not show mutagenicity with bacterial strain *Salmonella typhimurium* types *TA 98, TA 100, TA 1535,* and *TA 1538* in the assayed range.

3.8. DNA Binding Properties. It was reported that DNA binding mode and affinity are affected by a number of factors, such as planarity of ligands [41], the coordination geometry, the ligand donor atom type [42], the metal ion type, and its flexible valence [43]. The UV binding of the complexes **1–3** to the calf thymus (CT) DNA has been studied by electronic absorption spectral technique.

The intrinsic binding constant (K_b) value was $3.99(\pm0.04) \times 10^6 \, M^{-1}$ for complex **2** (Figure 5). The complexes **1** and **3** did not show binding affinity to CT-DNA due to lack of planarity. The experimental values of K_b revealed that complex **2** binds to DNA via intercalative mode, and this may be due to the presence of the phenanthroline ring in the structure.

The emission spectral method is used to study the relative binding of the complexes to CT-DNA. The emission intensity of ethidium bromide (EB) is used as a spectral probe. EB shows reduced emission intensity in buffer solution because of solvent quenching and an enhancement of the emission intensity when intercalatively bound to DNA. The binding of
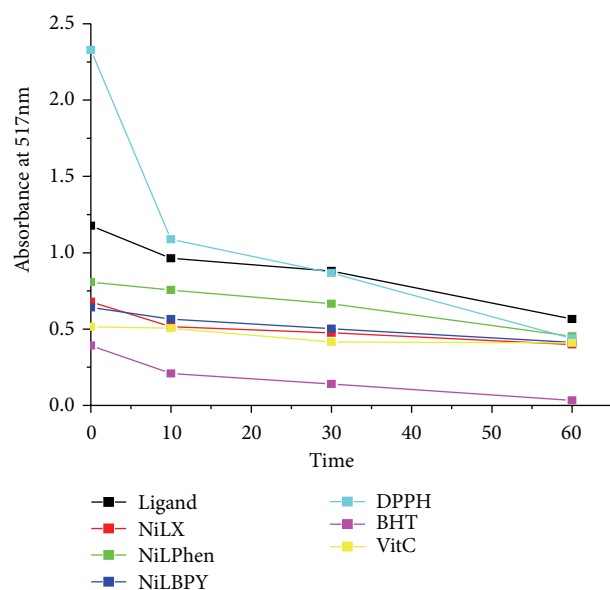

FIGURE 4: The comparative time-dependent antioxidant activity of complexes **1**, **2**, and **3** and standards.
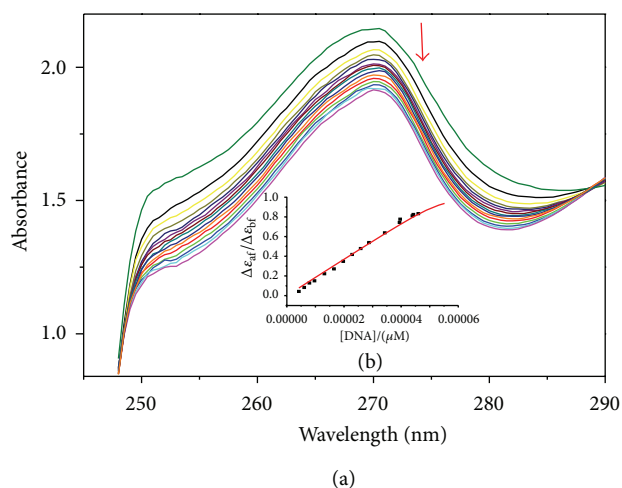

FIGURE 5: (a) Absorption spectral traces showing the decrease in absorption intensity on gradual addition of CT-DNA (270 μM) in aliquots to the solution of complex **2** (60 μM) in 5 mM tris-HCl buffer (pH 7.2) at 25°C (shown by arrow). (b) Inset shows plot of [DNA]/($\varepsilon_a - \varepsilon_f$) versus [DNA] for absorption titration of CT-DNA with complex **2**.

the complexes to DNA decreases the emission intensity of EB (Figures 6(a), 6(b), and 6(c)). The relative binding propensity of the complexes to DNA is measured from the extent of reduction in the emission intensity (Figure 7). The apparent binding constant (K_{app}) values for **1, 2,** and **3** are given in Table 7. The phen complex showed significantly higher K_{app} values than those of the bpy and bis ligand complexes. The bis ligand complex is a poor binder to DNA.

The nature of the binding of the complexes to CT-DNA was further investigated by DNA melting experiment. Thermal behavior of the DNA in the presence of metal
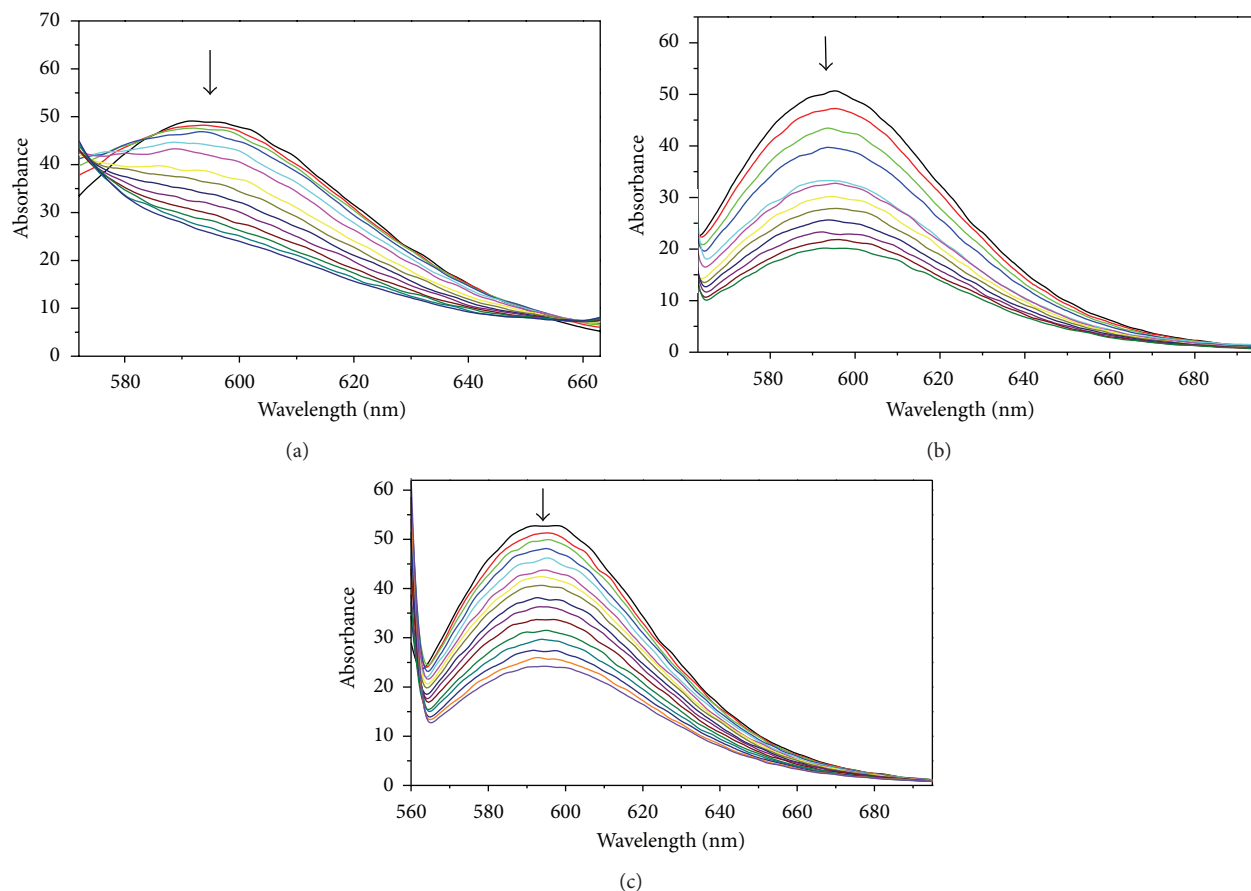
(a)

(b)

(c)

FIGURE 6: The emission spectral changes on addition of complexes **1** (a), **2** (b), and **3** (c) to the CT-DNA bound to ethidium bromide (shown by arrow).
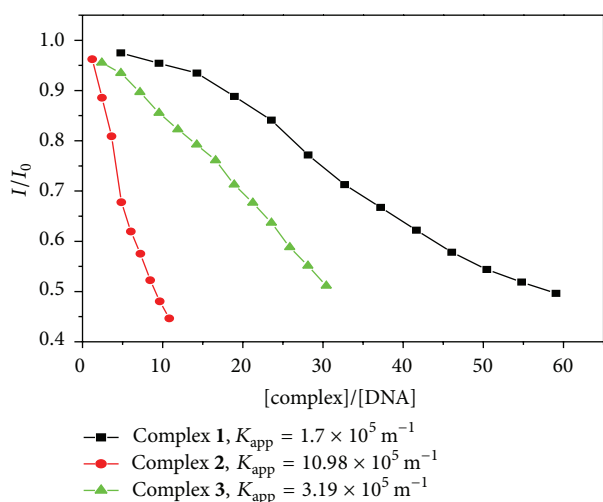

FIGURE 7: The effect of addition of metal complexes **1**, **2**, and **3** to the emission intensity CT-DNA bound ethidium bromide in a 5 mM tris-HCl (pH = 7.2) at 25°C.

TABLE 7: Intrinsic binding, apparent DNA binding, and melting temperature studies.

Complexes	[a]K_b/M^{-1}	[b]K_{app}/M^{-1}	[c]ΔT_m °C
1		1.7×10^5	$\cdots$
2	3.99×10^6	10.98×10^5	$+0.8$
3		3.19×10^5	-0.4

[a]Intrinsic binding constant from absorption spectral method.
[b]Apparent binding constant from competitive binding assay by emission method.
[c]Changes in melting temperature of CT-DNA.

complexes can give insight into their conformational changes and information about the interaction strength with DNA. DNA melting is observed when ds DNA molecules are heated and separated into two single strands; it occurs due to a disruption of the intermolecular forces, such as π stacking and hydrogen bonding interactions, between DNA base pairs.

A classical intercalator such as EB stabilizes the duplex DNA, causing the DNA to melt at a higher temperature [44]. The melting temperature of CT-DNA in the absence of any added complex was found to be 65.5°C in our experimental conditions. Under the same set of conditions, in the presence of all the complexes, they gave ΔT_m values ranging from 0.4 to +0.8°C indicating primarily DNA groove binding propensity of the complexes. The phen complex **2** with a relatively high ΔT_m value of +0.8°C could have a partial intercalative

TABLE 8: Selected cleavage data of SC pUC19 by ligand and its complexes **1**, **2**, and **3**.

Lane no.	Conditions	[Complex] μM	[a]SC%	[b]NC%
1	DNA control	—	97	3
2	DNA + Ligand + H$_2$O$_2$	60	92	8
3	DNA + Ligand + MPA	60	93	7
4	DNA + **1** + MPA	60	90	10
5	DNA + **2** + MPA	60	87	13
6	DNA + **3** + MPA	60	89	11
7	DNA + **1** + H$_2$O$_2$	60	78	22
8	DNA + **2** + H$_2$O$_2$	60	65	35
9	DNA + **3** + H$_2$O$_2$	60	75	25

[a]SC: supercoiled DNA.
[b]NC: nicked circular DNA.

mode of DNA binding with the planar ring of 1,10-phen intercalating to the DNA base pairs.

3.9. DNA Cleavage Studies. The oxidative DNA cleavage activity of the complexes in the presence of oxidizing agent hydrogen peroxide (H$_2$O$_2$, 50 mM) is investigated by agarose gel electrophoresis using supercoiled (SC) plasmid pUC19 DNA (0.2 μg, 33.3 μM NP) in 50 mM tris-HCl/50 mM NaCl buffer (pH 7.2), and the selected DNA cleavage data are given in Table 8. The phen complex **2** (60 μM) shows moderate "chemical nuclease" activity, and 35% conversion of the SC (form I) to its nicked-circular form (NC, form II) of DNA is observed. Control experiments with H$_2$O$_2$ or the complexes alone did not show any apparent conversion of SC to its nicked-circular (NC) form (Figure 8). The bpy complex **3** and bis ligand complex **1** are inactive due to their poor binding ability to DNA. The pathways involved in the DNA cleavage reactions are believed to be analogous to those proposed by Sigman and coworkers for the chemical nuclease activity of bis(phen)copper species (Scheme 1) [45, 46]. Based on the mechanistic studies it is observed that chemical nuclease activity is high in oxidizing condition compared to reducing condition.

4. Conclusions

Three new Ni(II) complexes having N,S-donor ligand and N,N-donor heterocyclic bases are prepared and characterized. The complex **1** was structurally characterized by X-ray crystallography, and the structure shows the square planar geometry. The free radical scavenging assay results showed that complex **1** posseses significant activity when compared to complexes **2** and **3**. The biological studies showed that the ligand and its complexes exhibited significant and different biological activities and also the prepared compounds are nonmutagenic. They may be potential commercial antioxidants because of their nonmutagenic and nontoxic nature. The DNA interaction of the new complexes was evaluated by absorption, emission, and melting temperature methods, and the results suggested that the binding affinity of the complexes increases with the presence of planar ligand in the molecule.

$$Ni^{II}(L)_2/(LB) + DNA \longrightarrow Ni^{II}(L)_2/(LB)----DNA$$

$$\downarrow MPA/H_2O_2$$

$$\text{Nicked DNA} \longleftarrow \{OH^\bullet\} \overset{O_2}{\longleftarrow} Ni^{I/III}(L)_2/(LB)----DNA$$
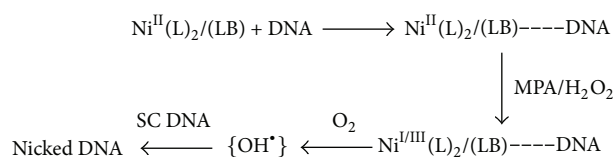
SCHEME 1: Proposed mechanistic pathway for the chemical nuclease activity of complexes in tris-buffer medium.
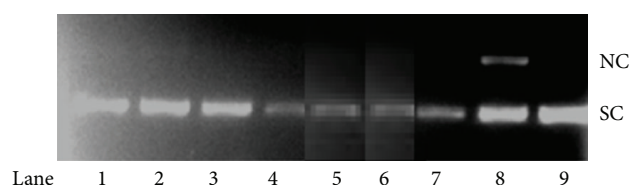
FIGURE 8: Gel electrophoresis diagram showing the cleavage of SC pUC19 DNA by complexes **1**, **2**, and **3** and ligand in 50 mm tris-HCL/50 mm NaCl buffer (pH 7.2) in the presence oxidizing and reducing agents.

The nickel(II) complexes with planar phenanthroline bases show moderate DNA binding and cleavage ability.
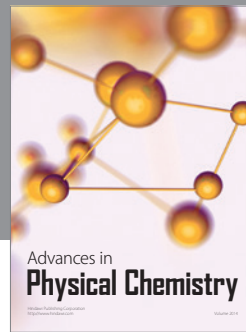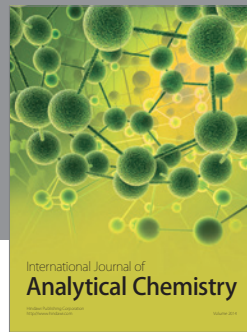
Acknowledgments

References

[1] N. Raman, S. Johnson Raja, and A. Sakthivel, "Transition metal complexes with Schiff-base ligands: 4-Aminoantipyrine based derivatives—a review," *Journal of Coordination Chemistry*, vol. 62, no. 5, pp. 691–709, 2009.

[2] M. A. Ali, N. E. H. Ibrahim, R. J. Butcher, J. P. Jasinski, J. M. Jasinski, and J. C. Bryan, "Synthesis and characterization of some four-and five-coordinate copper(II) complexes of 6-methyl-2-formylpyridinethiosemicarbazone (HNNS) and the X-ray crystal structures of the [Cu(NNS)(CH$_3$COO)(H$_2$O)] and [Cu(HNNS)(H$_2$O)(SO$_4$)]·H$_2$O complexes," *Polyhedron*, vol. 17, no. 11-12, pp. 1803–1809, 1998.

[3] Y.-J. Kim, S.-O. Kim, Y.-I. Kim, and S.-N. Choi, "A mimic molecule of blue copper protein active site [(−)-sparteine-*N*,*N'*](maleonitriledithiolato-*S*,*S'*)copper(II)," *Inorganic Chemistry*, vol. 40, no. 17, pp. 4481–4484, 2001.

[4] M. M. van Dyke and P. B. Dervan, "Echinomycin binding sites on DNA," *Science*, vol. 225, no. 4667, pp. 1122–1127, 1984.

[5] B. G. Patil, B. R. Havinale, J. M. Shallom, and M. P. Chitnis, "Syntheses and spectroscopic studies of potential antitumor copper(II) complexes with 5-phenylazo-3-methoxy salicylidene thiosemicarbazone and N4 substituted thiosemicarbazones," *Journal of Inorganic Biochemistry*, vol. 36, no. 2, pp. 107–113, 1989.

[6] P. V. Bernhardt, J. Mattsson, and D. R. Richardson, "Complexes of cytotoxic chelators from the dipyridyl ketone isonicotinoyl hydrazone (HPKIH) analogues," *Inorganic Chemistry*, vol. 45, no. 2, pp. 752–760, 2006.

[7] M. Akbar Ali and S. E. Livingstone, "Metal complexes of sulphur-nitrogen chelating agents," *Coordination Chemistry Reviews*, vol. 13, no. 2-3, pp. 101–132, 1974.

[8] C. Costello, T. Karpanen, P. A. Lambert et al., "Thiosemicarbazones active against Clostridium difficile," *Bioorganic and Medicinal Chemistry Letters*, vol. 18, no. 5, pp. 1708–1711, 2008.

[9] J. S. Sebolt, S. V. Scavone, and C. D. Pinter, "Pyrazoloacridines, a new class of anticancer agents with selectivity against solid tumors *in vitro*," *Cancer Research*, vol. 47, no. 16, pp. 4299–4304, 1987.

[10] S. Rekha and K. R. Nagasundara, "Complexes of the Schiff base derived from 4-aminophenyl benzimidazole and 2,2′-dehydropyrollidene-N-aldehyde with Zn (II), Cd (II) and Hg (II) halides," *Indian Journal of Chemistry A*, vol. 45, no. 11, pp. 2421–2425, 2006.

[11] D. Kovala-Demertzi, A. Papageorgiou, L. Papathanasis et al., "*In vitro* and *in vivo* antitumor activity of platinum(II) complexes with thiosemicarbazones derived from 2-formyl and 2-acetyl pyridine and containing ring incorporated at N(4)-position: synthesis, spectroscopic study and crystal structure of platinum(II) complexes with thiosemicarbazones, potential anticancer agents," *European Journal of Medicinal Chemistry*, vol. 44, no. 3, pp. 1296–1302, 2009.

[12] M. C. Rodrìguez-Argüelles, M. B. Ferrari, F. Bisceglie et al., "Synthesis, characterization and biological activity of Ni, Cu and Zn complexes of isatin hydrazones," *Journal of Inorganic Biochemistry*, vol. 98, no. 2, pp. 313–321, 2004.

[13] F. Liang, P. Wang, X. Zhou et al., "Nickle(II) and cobalt(II) complexes of hydroxyl-substituted triazamacrocyclic ligand as potential antitumor agents," *Bioorganic and Medicinal Chemistry Letters*, vol. 14, no. 8, pp. 1901–1904, 2004.

[14] J. Suh, "Synthetic artificial peptidases and nucleases using macromolecular catalytic systems," *Accounts of Chemical Research*, vol. 36, no. 7, pp. 562–570, 2003.

[15] R. T. Kovacic, J. T. Welch, and S. J. Franklin, "Sequence-selective DNA cleavage by a chimeric metallopeptide," *Journal of the American Chemical Society*, vol. 125, no. 22, pp. 6656–6662, 2003.

[16] D. S. Sigman, "Nuclease activity of 1,10-phenanthroline-copper ion," *Accounts of Chemical Research*, vol. 19, no. 6, pp. 180–186, 1986.

[17] D. S. Sigman, T. W. Bruice, A. Mazumder, and C. L. Sutton, "Targeted chemical nucleases," *Accounts of Chemical Research*, vol. 26, no. 3, pp. 98–104, 1993.

[18] K. E. Erkkila, D. T. Odom, and J. K. Barton, "Recognition and reaction of metallointercalators with DNA," *Chemical Reviews*, vol. 99, no. 9, pp. 2777–2795, 1999.

[19] R. M. Burger, "Cleavage of nucleic acids by bleomycin," *Chemical Reviews*, vol. 98, no. 3, pp. 1153–1169, 1998.

[20] B. M. Zeglis, V. C. Pierre, and J. K. Barton, "Metallo-intercalators and metallo-insertors," *Chemical Communications*, no. 44, pp. 4565–4579, 2007.

[21] M. A. S. Aslam, S.-U. Mahmood, M. Shahid, A. Saeed, and J. Iqbal, "Synthesis, biological assay *in vitro* and molecular docking studies of new Schiff base derivatives as potential urease inhibitors," *European Journal of Medicinal Chemistry*, vol. 46, no. 11, pp. 5473–5479, 2011.

[22] R. Rao, A. K. Patra, and P. R. Chetana, "Synthesis, structure, DNA binding and oxidative cleavage activity of ternary (L-leucine/isoleucine) copper(II) complexes of heterocyclic bases," *Polyhedron*, vol. 27, no. 5, pp. 1343–1352, 2008.

[23] N. Walker and D. Stuart, "An empirical method for correcting diffractometer data for absorption effects," *Acta Crystallographica A*, vol. 39, no. 1, pp. 158–166, 1983.

[24] G. M. Sheldrick, *SHELX-97, "Program For Crystal Structure Solution and Refinement"*, University of Göttingen, Göttingen, Germany, 1997.

[25] B. Matthäus, "Antioxidant activity of extracts obtained from residues of different oilseeds," *Journal of Agricultural and Food Chemistry*, vol. 50, no. 12, pp. 3444–3452, 2002.

[26] W. Brand-Williams, M. E. Cuvelier, and C. Berset, "Use of a free radical method to evaluate antioxidant activity," *Lebensmittel-Wissenschaft & Technologie*, vol. 28, no. 1, pp. 25–30, 1995.

[27] P. K. Mukherjee, R. Balasubramanian, K. Saha, B. P. Saha, and M. Pal, "Antibacterial efficiency of *Nelumbo nucifera* (nymphaeaceae) rhizomes extract," *Indian Drugs*, vol. 32, no. 6, pp. 274–276, 1995.

[28] D. M. Maron and B. N. Ames, "Revised methods for the *Salmonella mutagenicity* test," *Mutation Research*, vol. 113, no. 3-4, pp. 173–215, 1983.

[29] J. Marmur, "A procedure for the isolation of deoxyribonucleic acid from micro-organisms," *Journal of Molecular Biology*, vol. 3, pp. 208–218, 1961.

[30] M. E. Reichmann, S. A. Rice, C. A. Thomas, and P. Doty, "A further examination of the molecular weight and size of desoxypentose nucleic acid," *Journal of the American Chemical Society*, vol. 76, no. 11, pp. 3047–3053, 1954.

[31] A. Wolfe, G. H. Shimer Jr., and T. Meehan, "Polycyclic aromatic hydrocarbons physically intercalate into duplex regions of denatured DNA," *Biochemistry*, vol. 26, no. 20, pp. 6392–6396, 1987.

[32] J. B. LePecq and C. Paoletti, "A fluorescent complex between ethidium bromide And nucleic acids. Physical-chemical characterization," *Journal of Molecular Biolology*, vol. 27, pp. 87–106, 1967.

[33] S. Neidle, "DNA minor-grooverecognition by small molecules," *Natural Product Reports*, vol. 18, pp. 291–309, 2001.

[34] J. Bernadou, G. Pratviel, F. Bennis, M. Girardet, and B. Meunier, "Potassium monopersulfate and a water-soluble manganese porphyrin complex, [Mn(TMPyP)](OAc)5, as an efficient reagent for the oxidative cleavage of DNA," *Biochemistry*, vol. 28, no. 18, pp. 7268–7275, 1989.

[35] W. J. Geary, "The use of conductivity measurements in organic solvents for the characterisation of coordination compounds," *Coordination Chemistry Reviews*, vol. 7, no. 1, pp. 81–122, 1971.

[36] S. Chandra and U. Kumar, "Spectral studies of coordination compounds of cobalt(II) with thiosemicarbazone of heterocyclic ketone," *Spectrochimica Acta A*, vol. 62, no. 4-5, pp. 940–944, 2005.

[37] N. S. Youssef and K. H. Hegab, "Synthesis and characterization of some transition metal complexes of thiosemicarbazones derived from 2-acetylpyrrole and 2-acetylfuran," *Synthesis and Reactivity in Inorganic, Metal-Organic and Nano-Metal Chemistry*, vol. 35, no. 5, pp. 391–399, 2005.

[38] C. Sanchez-Moreno, J. A. Larrauri, and F. Saura-Calixto, "A procedure to measure the antiradical efficiency of polyphenols," *Journal of the Science of Food and Agriculture*, vol. 76, no. 2, pp. 270–276, 1998.

[39] A. R. Burkanudeen, R. S. Azarudeen, M. A. R. Ahamed, and W. B. Gurnule, "Kinetics of thermal decomposition and antimicrobial screening of terpolymer resins," *Polymer Bulletin*, vol. 67, no. 8, pp. 1553–1568, 2011.

[40] M. S. Refat and N. M. El-Metwaly, "Spectral, thermal and biological studies of Mn(II) and Cu(II) complexes with two thiosemicarbazide derivatives," *Spectrochimica Acta A*, vol. 92, pp. 336–346, 2012.

[41] C. V. Kumar, J. K. Barton, and N. J. Turro, "Photophysics of ruthenium complexes bound to double helical DNA," *Journal of the American Chemical Society*, vol. 107, no. 19, pp. 5518–5523, 1985.

[42] S. Mahadevan and M. Palaniandavar, "Spectroscopic and voltammetric studies of copper (II) complexes of bis(pyrid-2-yl)-di/trithia ligands bound to calf thymus DNA," *Inorganica Chimica Acta*, vol. 254, no. 2, pp. 291–302, 1997.

[43] M. Asadi, E. Safaei, B. Ranjbar, and L. Hasani, "Thermodynamic and spectroscopic study on the binding of cationic ZD(II) and Co(II) tetrapyridinoporphyrazines to calf thymus DNA: the role of the central metal in binding parameters," *New Journal of Chemistry*, vol. 28, no. 10, pp. 1227–1234, 2004.

[44] J. M. Kelly, A. B. Tossi, D. J. Mcconnell, and C. Ohuigin, "A study of the interactions of some polypyridylruthenium(II) complexes with DNA using fluorescence spectroscopy, topoisomerisation and thermal denaturation," *Nucleic Acids Research*, vol. 13, no. 17, pp. 6017–6034, 1985.

[45] O. Zelenko, J. Gallagher, and D. S. Sigman, "Scission of DNA with Bis(1,10-phenanthroline)copper without Intramolecular Hydrogen Migration," *Angewandte Chemie (International Edition)*, vol. 36, no. 24, pp. 2776–2778, 1997.

[46] D. S. Sigman, "Chemical nucleases," *Biochemistry*, vol. 29, no. 39, pp. 9097–9105, 1990.